

Recombinant immunotoxin targeting GPC3 is cytotoxic to H446 small cell lung cancer cells

EWELINA RODAKOWSKA^{1*}, AURELIA WALCZAK-DRZEWIECKA^{2*}, MARTA BOROWIEC³,
MICHAL GORZKIEWICZ^{2,4}, JOANNA GRZESIK³, MARCIN RATAJEWSKI⁵, MICHAL ROZANSKI²,
JAROSLAW DASTYCH², KRZYSZTOF GINALSKI³ and LESZEK RYCHLEWSKI¹

¹BioInfoBank Institute, 61-809 Poznan; ²Laboratory of Cellular Immunology, Institute of Medical Biology, Polish Academy of Sciences, 93-232 Lodz; ³Laboratory of Bioinformatics and Systems Biology, Centre of New Technologies, University of Warsaw, 02-89 Warsaw; ⁴Department of General Biophysics, Faculty of Biology and Environmental Protection, University of Lodz, 90-236 Lodz; ⁵Laboratory of Epigenetics, Institute of Medical Biology, Polish Academy of Sciences, 93-232 Lodz, Poland

Received July 23, 2020; Accepted December 9, 2020

DOI: 10.3892/ol.2021.12483

Abstract. Glypican-3 (GPC3) is a cell membrane glycoprotein that regulates cell growth and proliferation. Aberrant expression or distribution of GPC3 underlies developmental abnormalities and the development of solid tumours. The strongest evidence for the participation of GPC3 in carcinogenesis stems from studies on hepatocellular carcinoma and lung squamous cell carcinoma. To the best of our knowledge, the role of the GPC3 protein and its potential therapeutic application have never been studied in small cell lung carcinoma (SCLC), despite the known involvement of associated pathways and the high mortality caused by this disease. Therefore, the aim of the present study was to examine GPC3 targeting for SCLC immunotherapy. An immunotoxin carrying an anti-GPC3 antibody (hGC33) and *Pseudomonas aeruginosa* exotoxin A 38 (PE38) was generated. This hGC33-PE38 protein was overexpressed in *E. coli* and purified. ADP-ribosylation activity was tested *in vitro* against eukaryotic translation elongation factor 2. Cell internalisation ability was confirmed by confocal microscopy. Cytotoxicity was analysed by treating

liver cancer (HepG2, SNU-398 and SNU-449) and lung cancer (NCI-H510A, NCI-H446, A549 and SK-MES1) cell lines with hGC33-PE38 and estimating viable cells number. A BrdU assay was employed to verify anti-proliferative activity of hGC33-PE38 on treated cells. Fluorescence-activated cell sorting was used for the detection of cell membrane-bound GPC3. The hGC33-PE38 immunotoxin displayed enzymatic activity comparable to native PE38. The protein was efficiently internalised by GPC3-positive cells. Moreover, hGC33-PE38 was cytotoxic to HepG2 cells but had no effect on known GPC3-negative cell lines. The H446 cells were sensitive to hGC33-PE38 (IC₅₀, 70.6±4.6 ng/ml), whereas H510A cells were resistant. Cell surface-bound GPC3 was abundant on the membranes of H446 cells, but absent on H510A. Altogether, the present findings suggested that GPC3 could be considered as a potential therapeutic target for SCLC immunotherapy.

Introduction

The glypican-3 (GPC3) protein has emerged as a novel, promising target for cancer immunotherapy (1). GPC3 is a member of the membrane-bound heparan sulphate proteoglycan (glypican) family (2). The C-terminal fragment of GPC3 is anchored to the cell membrane via a glycosylphosphatidylinositol (GPI) anchor, whereas its N-terminus can be released into the extracellular matrix (3,4). This modular structure enables GPC3 to function as a receptor interacting with several regulatory molecules. The expression of GPC3 is relatively high during embryonic development and is precisely regulated in a tissue- and stage-specific manner (5), suggesting a role for GPC3 in morphogenesis and embryonic development. After birth, GPC3 is rarely detectable in healthy tissue. Previous studies demonstrated that GPC3 was overexpressed in hepatocellular carcinoma (HCC) and that its expression could serve as a potential diagnostic marker and prognostic factor for this disease (1,6-9). The role of GPC3 in HCC pathogenesis and development is not fully understood, and few underlying mechanisms have been proposed. Cell membrane-bound GPC3 can interact with growth factors; for

Correspondence to: Ms. Ewelina Rodakowska, BioInfoBank Institute, Sw. Marcin 80/82, lok. 355, 61-809 Poznan, Poland
E-mail: rodakowska.e@gmail.com

*Contributed equally

Abbreviations: GPC3, glypican-3; HCC, hepatocellular carcinoma; SCLC, small cell lung carcinoma; LSCC, lung squamous cell carcinoma; LAD, lung adenocarcinoma; RIT, recombinant immunotoxin; Hh, Hedgehog; mAb, monoclonal antibody; PE38, *Pseudomonas aeruginosa* exotoxin A 38

Key words: glypican-3, immunotoxin, small cell lung carcinoma, Wnt/β-catenin pathway, hepatocellular carcinoma, immunotherapy

example, it binds Wnt and stimulates Wnt/ β -catenin signalling, leading to HCC development (10). The involvement of GPC3 in the Yap (Yes-associated protein) and Hedgehog (Hh) signalling pathways was described in other cancer types and developmental processes (11). Filmus and Capurro (12) proposed that GPC3 could stimulate cell proliferation in tumours with a dominant influence of the Wnt signalling and inhibit proliferation in tumours with predominant Hh signalling. Evaluating the potential use of the GPC3 antigen would provide further insight into the targeted therapy of other cancer types. Aside from HCC, the overexpression has been observed in several tumour types, especially in embryonic carcinoma, yolk sac tumours, non-small cell lung cancer and thyroid cancer (13-25). Conversely, in some tumours, the expression of GPC3 is decreased compared with normal tissue (10,26-29).

In lung cancer, a major contributor to cancer-associated deaths worldwide, the role of GPC3 may be cell-type dependent and remains poorly understood. The presence of GPC3 in healthy lung tissue has not been reported. GPC3 expression is significantly increased in lung squamous cell carcinoma (LSCC), both at the mRNA and the protein levels (24,30-33). Typically, GPC3 presence is detected in more than half of analysed specimens from patients with LSCC and LSCC cell lines (24,30-33). Importantly, GPC3 levels correlate inversely with LSCC differentiation grade, and positively with metastasis and disease progression (24). Li *et al* (33) demonstrated that GPC3 could represent a rational target in immunotherapy for LSCC. These authors developed a strategy based on (GPC3)-redirected chimeric antigen receptor (CAR)-engineered T lymphocytes that is currently under evaluation in a phase-I clinical trial (33,34). By contrast, the GPC3 protein is rarely detected on the surface of lung adenocarcinoma (LAD) cells, where it is expressed at low mRNA levels (24,30,31). To the best of our knowledge, there are no reports describing the role of GPC3 in the exceptionally malignant small cell lung carcinoma (SCLC). Therefore, the aim of the present study was to determine whether the GPC3 protein could represent a potential target for SCLC immunotherapy.

In this study, an effective and highly specific PE38-based immunotoxin comprising the humanised mouse monoclonal antibody hGC33 against a C-terminal epitope of GPC3 was used (35). Recombinant immunotoxins (RITs) are chimeric proteins composed of a portion of a monoclonal antibody (mAb) fused to a portion of bacterial, plant or animal toxin. Thus, the variable fragment (Fv) of the mAb directs the toxin to the cells expressing the target antigen. As a result, the cell surface-bound immunotoxin is internalised via receptor-dependent endocytosis and translocates to the cytoplasm where it causes cell death, mostly through protein synthesis inhibition (36-38). Gao *et al* (39) developed immunotoxin variants based on a *P. aeruginosa* exotoxin A fragments (PE38 variant) fused to several different anti-GPC3 antibodies (39,40). The results obtained *in vitro* and in mouse xenograft experiments demonstrated that anti-GPC3 immunotoxins may become very potent antitumor therapeutics for HCC therapy (39,40). The aim of the present study was to evaluate the GPC3-directed cytotoxicity on two SCLC cell lines, NCI-H510A and NCI-H446, chosen for their relatively high GPC3 mRNA levels (41). The use of the GPC3 antigen as a target for immunotoxin in the SCLC cell lines is described for the first time. The present findings suggested a possible

role for GPC3 in SCLC and indicated that this antigen might represent a useful candidate for SCLC immunotherapy.

Materials and methods

Protein overexpression and purification. The coding sequence of the hGC33-PE38 immunotoxin was designed by linking two functional domains: i) the sequence encoding the hGC33 antibody at the N-terminus; and ii) a truncated exotoxin A fragment lacking its native binding moiety and a fragment of the domain Ib (referred to as PE38) at the C-terminus (42). The last, terminal codon for lysine of PE38 was deleted resulting in the C-terminal REDL sequence. The GPC3-binding domain sequence encoded the single-chain Fv humanised mouse monoclonal antibody named hGC33 according to the hGC33VHk/hGC33VL_a_Arg variant created by Nakano *et al* (35). Between the hGC33 antibody and PE38, a short linker encoding the N-ASGGGGSGGGTSGGGGSA-C sequence was inserted. In some experiments, the native PE38 exotoxin A (referred to as N-PE38 thereafter) was used as a control. The production and purification of N-PE38 and hGC33-PE38 were performed in the same way.

The genes encoding the hGC33-PE38 immunotoxin and N-PE38 were codon-optimised for expression in *E. coli* and synthesised commercially by Invitrogen (Thermo Fisher Scientific, Inc.). The synthetic coding fragments were cloned into the pET28SUMO expression vector, which was previously produced in our laboratory by the insertion of the SUMO protein coding sequence into the pET28a (Novogene Co., Ltd.). As a result, the proteins of interest were fused to a His-tagged SUMO. The constructs were sequenced to confirm sequence identity and correct gene orientation.

The NiCo21(DE3) chemocompetent *E. coli* strain was transformed with expression vectors by heat shock and placed onto Agar plates supplemented with 1% glucose and kanamycin. The preculture was inoculated with a single colony and grown in TB medium (Sigma-Aldrich; Merck KGaA) for 16 h at 37°C. Fresh TB medium was warmed to 37°C and inoculated with seed culture at a culture:medium ratio of 1:100. Protein overexpression was induced with 0.5 mM IPTG when OD₆₀₀ reached 0.4 and further grown for 14 h at 23°C. At the end of the incubation, bacteria were collected by centrifugation. The bacterial pellet was suspended in lysis buffer (50 mM NaH₂PO₄; 300 mM NaCl; 20 mM imidazole; 10% glycerol; 0.5 mM PMSF; 5 mM β -mercaptoethanol; 1 mg/ml lysozyme; 0.05% Triton X-100; 5 U/ml Benzonase[®]; pH 8.0). Re-suspended cells were sonicated and centrifuged at 15,000 x g at 4°C for 20 min. The supernatant containing the protein of interest was collected and immediately processed. Protein was purified on two connected chromatography columns, the first containing chitin resin (New England Biolabs, Inc.) and the second filled with NiNTA Superflow resin (Qiagen GmbH). Columns were previously equilibrated using a lysis buffer (50 mM NaH₂PO₄, 300 mM NaCl, 20 mM imidazole, 10% glycerol, pH 8.0). The supernatant was loaded with a constant flow rate of 0.1 ml/min. After protein binding, columns were washed using 8 column volumes of lysis buffer and were disconnected afterwards. The single NiNTA column was then washed with high-salt buffer (50 mM NaH₂PO₄; 2000 mM NaCl; 20 mM imidazole; 10% glycerol; pH 8.0) to

remove non-specifically bound material. The proteins were eluted in gradient-elution mode with buffer (50 mM NaH₂PO₄; 300 mM NaCl; 500 mM imidazole; 10% glycerol; pH 8.0). The collected fractions were pooled and SUMO protease was used to remove the SUMO-tag. After SUMO-tag removal, the protein of interest was filtered and loaded on a size exclusion column (HiLoad Superdex 200; GE Healthcare Life Sciences) and equilibrated with PBS (pH 7.4), containing 10% glycerol. The fractions containing the hGC33-PE38 immunotoxin were pooled and concentrated on a Vivaspin Turbo concentrator (Sigma-Aldrich; Merck KGaA). Protein purity was assessed by densitometry and through the use of a Bradford protein assay (Bio-Rad Laboratories, Inc.). The integrity and molecular weight of the immunotoxin were analysed by 10% SDS-PAGE in reducing conditions and by western blotting. For western blotting, 50 ng protein/lane was separated via 10% SDS-PAGE under reducing conditions and then transferred onto a PVDF membrane using a semi-dry electrophoretic transfer. Prior to immunodetection, the membrane was blocked overnight with SuperBlock (TBS) Blocking Buffer (Thermo Fisher Scientific, Inc.) at room temperature. Subsequently, the membrane was incubated with an anti-Pseudomonas exotoxin A-specific primary antibody (1:5,000; cat. no. P2318; Sigma-Aldrich; Merck KGaA) for 1 h at room temperature with gentle agitation. The primary antibody was detected using a goat anti-rabbit HRP-conjugated secondary antibody (1:2,000; cat. no. A6154; Sigma-Aldrich; Merck KGaA) by incubating for 1 h at room temperature with gentle agitation. Bounded antibodies were visualized using ECL Western Blotting Detection Reagents (GE Healthcare Life Sciences) and chemiluminescent signals were analyzed using a molecular imager (Bio-Rad Laboratories, Inc.).

ADP-ribosylation assay. The ADP-ribosylation activities of the hGC33-PE38 and N-PE38 were measured using a solid-phase assay against *S. cerevisiae* eEF2 as a substrate, as previously described (43). The ADP-ribosylation capacity was measured by rapid detection using the western blotting method with HRP-conjugated streptavidin against biotin-labelled ADP-ribose covalently bound to eEF2 as described by Borowiec *et al* (43). The EC₅₀ values were calculated from dose-response curves using the GraphPad Prism 5 software (GraphPad Software, Inc.).

ELISA. A clear, flat-bottomed, polystyrene, 96-well plate was coated overnight at 4°C with recombinant human glypican-3 protein (R&D Systems, Inc.) at increasing concentrations. As a negative control, wells were also coated with 3% (w/v) Bovine Serum Albumin (BSA) in wash buffer. The plate was subsequently washed three times with PBS + 0.1% Tween-20 to remove unbound protein and blocked with 3% BSA with 0.1% Tween-20 for 3 h at room temperature. Then, the plate was washed three times with PBS + 0.1% Tween-20. In the next step, 1 µg/ml immunotoxin was added to each well. The plate was incubated for 1 h at room temperature, and subsequently washed three times with PBS + 0.1% Tween-20. The plate was then incubated with anti-*P. aeruginosa* exotoxin A-specific antibodies (1:250,000; cat. no. P2318; Sigma-Aldrich; Merck KGaA) for 1 h at room temperature and washed three times with PBS + 0.1% Tween-20. The primary antibody was labelled using an anti-rabbit HRP-conjugated

secondary antibody (1:2,000; cat. no. P0448; Dako; Agilent Technologies, Inc.) for 1 h at room temperature and detected using Super Signal ELISA Pico Chemiluminescent Substrate (cat. no. 37069; Thermo Fisher Scientific, Inc.). The incubation with the substrate was performed for 30 min at room temperature. The absorbance was then measured at 450 nm using a Sunrise Tecan microplate reader (Tecan Group, Ltd.).

Cell lines. The human liver cancer cell lines HepG2, SNU-398 and SNU-449; SCLC cell lines NCI-H510A (HTB-184), NCI-H446 (HTB-171) and LAD A549, were purchased from American Type Culture Collection (ATCC). The SNU-398, SNU-449, NCI-H446 cell lines were cultured in RPMI-1640 medium (Thermo Fisher Scientific, Inc.) containing 10% heat-inactivated FBS (Thermo Fisher Scientific, Inc.). The NCI-H510A cell line was cultured in F-12K medium (ATCC) supplemented with 10% FBS. The HepG2 and A549 cell lines were maintained under standard conditions in Dulbecco's modified Eagle's medium (Thermo Fisher Scientific, Inc.) supplemented with 10% FBS. The cells were subcultured when they reached the exponential phase. All cell cultures were free of mycoplasma which was confirmed by routine test using the MycoAlert™ Mycoplasma Detection kit (Lonza Group, Ltd.).

Internalisation studies

Alexa Fluor® 488 dye staining and visualization. The fluorescent labelling of the hGC33-PE38 immunotoxin was performed using Alexa Fluor 488 Dye (Thermo Fisher Scientific, Inc.) according to the manufacturer's recommendations. A549 and HepG2 cells were incubated at 37°C with 1.5 µg/ml of fluorescently labelled protein for 3 h. The cells were then fixed in 4% formaldehyde for 10 min at room temperature, then stained for 20 min at room temperature with NucRed Live 647 ReadyProbes Reagent (Thermo Fisher Scientific, Inc.) for nuclei visualisation, and Alexa Fluor 594 Phalloidin (Thermo Fisher Scientific, Inc.) for actin visualisation, both according to the manufacturer's protocol. For fluorescence visualisation, the Nikon C1 confocal microscope was used (Nikon Corporation; magnification, x60).

ATTO 542 NHS-ester staining and visualization. The hGC33-PE38 immunotoxin was covalently stained with the fluorescent dye ATTO 542 NHS-ester (Atto-Tec GmbH) according to manufacturer's protocol. NCI-H446 and NCI-H510A cells were incubated with 4.5 µg/ml ATTO 542-stained hGC33-PE38 immunotoxin in complete medium for 1 h at 37°C. Subsequently, cells were washed twice with complete medium for 10 min each and resuspended in HBSS with 1 µM calcein-AM (Thermo Fisher Scientific, Inc.) and 4 µM Hoechst 33342 (Thermo Fisher Scientific, Inc.). After another 20-min incubation at 37°C, a portion of cells were transferred onto the SensoPlate. The plate was centrifuged for 3 min at 300 x g at room temperature and the cells were then imaged. Images were obtained using the Nikon Eclipse TE2000-S inverted microscope with and Plan-Apochromat 60x/1.4 Oil DIC N2 objective and a Nikon C1 confocal attachment (all from Nikon Corporation).

Cytotoxicity assay. In order to evaluate the cytotoxicity of the hGC33-PE38 immunotoxin, a neutral red uptake assay was performed (44). For each line tested, cells were seeded into

96-well plates in triplicate at a density of 1.5×10^4 cells/well. After 24 h, the cells were treated with increasing concentrations of hGC33-PE38 and incubated for another 48 h. Cells were also treated with 20 $\mu\text{g/ml}$ of CHX as a control to assess their sensitivity to the inhibition of protein synthesis. SDS (200 $\mu\text{g/ml}$) was also used as a standard cell membrane-damaging agent. After a 48-h incubation with a cytotoxic agent, the medium was removed and cells were washed with cold PBS. The cells were then incubated for 3 h with 50 $\mu\text{g/ml}$ of neutral red (Sigma-Aldrich; Merck KGaA) in HBSS. The neutral red solution was removed, and the cells washed with PBS. Subsequently, the cell-bound dye was extracted using a solution containing 50% ethanol and 1% acetic acid by gentle shaking for 10 min at room temperature. Absorbance at 550 nm was measured using a Sunrise microplate reader (Tecan Group, Ltd.). The half-maximal inhibitory concentration (IC_{50}) values were calculated based on linear dose-response curves using the GraphPad Prism 5 software.

Cell proliferation assay. For the determination of the effects of hGC33-PE38 immunotoxin on cell proliferation, a BrdU Cell Proliferation ELISA kit (Abcam; cat. no. ab126556) was used. NCI-H446 cells were seeded on clear 96-wells plates at a density of 1×10^4 cells/well. The following day, cells were treated with increasing concentrations of hGC33-PE38 immunotoxin and incubated for an additional 48 h. BrdU was added to wells 24 h before the end of the experiment. The cells were then fixed at room temperature for 30 min using Fixing Solution (part of the aforementioned BrdU Cell Proliferation ELISA kit), and the subsequent procedure was done according to the manufacturer's protocol. The absorbance of 450 nm was measured on an Infinite 200 PRO plate reader.

Microarray data analysis. The publicly available microarray results were analysed for GPC3 expression by performing a search on the Expression Atlas site (<https://www.ebi.ac.uk/gxa/experiments/E-MTAB-2706>) using 'GPC3' as the gene name. The chosen diseases were 'lung adenocarcinoma', 'lung adenosquamous', 'small cell lung carcinoma' and 'squamous cell lung carcinoma', which resulted in the automatic selection of 67 cell lines. The applied expression value was 0.5. The obtained results were viewed as fragments per kilobase of exon model per million reads mapped (FPKM; normalised within each set of biological replicates). Reads below the minimum quality threshold were automatically discarded. The primary data are available through the Array Express Archive (www.ebi.ac.uk/arrayexpress/) under the accession number: E-MTAB-2706.

Reverse transcription-quantitative (RT-q) PCR. Total RNA from NCI-H446 and NCI-H510A cells was isolated using TRIzol[®] reagent (Invitrogen; Thermo Fisher Scientific, Inc.) according to the manufacturer's instruction. Total RNA (5 μg) from each sample was reverse transcribed for 10 min at 25°C followed by 15 min at 50°C using the Maxima First Strand cDNA Synthesis kit for RT-qPCR (Thermo Fisher Scientific, Inc.). The qPCR step was performed using LightCycler[®] 480 SYBR Green I Master (Roche Diagnostics) on the Light Cyclor 480 Real-time PCR Instrument (Roche Diagnostics). Reaction conditions were as follows: Initial denaturation at 95°C for 5 min; 35 cycles at 95°C for 10 sec, 55°C for 10 sec and 72°C

for 20 sec; melting curve at 95°C for 30 sec, 72°C for 45 sec and 97°C continuous; and cooling at 40°C for 15 sec. The following primers were used: i) GPC3-forward, 5'-TGGAGT CAGGCTTGGGTAGT-3' and reverse, 5'-ATTCAGAATGCT GCGGTTTT-3'; ii) β -catenin-forward, 5'-CATTACAACCTCC CACAACC-3' and reverse, 5'-CAGATAGCACCTTCAG CAC-3' (45); iii) hydroxymethylbilane synthase (HMBS)-forward, 5'-GGCAATGCGGCTGCAA-3' and reverse, 5'-GGGTACCCACGCGAATCAC-3'; iv) hypoxanthine phosphoribosyltransferase 1 (HPRT)-forward, 5'-TGACACTG GCAAACAATGCA-3' and reverse, 5'-GGTCCTTTTCAC CAGCAAGCT-3'; v) ribosomal protein L13a (RPL13A)-forward, 5'-CCTGGAGGAGAAGAGGAAAGAGA-3' and reverse, 5'-TTGAGGACCTCTGTGTATTTGTCAA-3'. The HBMS, HPRT and RPL13A housekeeping genes were used to normalise the C_q values. The qPCR for each gene was carried out in triplicate. The obtained data was analysed using the $2^{-\Delta\Delta\text{C}_q}$ method (46). ΔC_t values were obtained by subtracting C_t of the studied genes from C_t of the geometric mean of reference genes (46). For presentation, ΔC_t , were recalculated into relative copy number values (number of copies of GPC3 or β -catenin per 1,000 copies of housekeeping genes).

Flow cytometry. HepG2, H446 and H510A cells were trypsinised into single-cell suspensions and then stained with mouse anti-human glypican-3 allophycocyanin-conjugated monoclonal antibody (10 $\mu\text{l}/10^6$ cells; cat. no. FAB2119A) or isotype control antibody IgG_{2A} (10 $\mu\text{l}/10^6$ cells; cat. no. IC003A) in Flow Cytometry Staining Buffer supplemented with BSA and sodium azide for 30 min at room temperature (all from R&D Systems, Inc.). Following incubation, excess antibody was removed by washing the cells twice in 2 ml Flow Cytometry Staining Buffer. Cell pellets were re-suspended in 200–400 μl Flow Cytometry Staining Buffer for flow cytometric analysis using a BD LSR Fortessa instrument (BD Biosciences).

Statistical analysis. Quantitative data are presented as the mean \pm SD of three independent replicates (or 95% confidence intervals for ADP-ribosylation activity). Statistical significance among groups was calculated using a one-way ANOVA followed by Dunnett's or Tukey's post hoc test. All statistical analyses were performed using GraphPad Prism 5 software (GraphPad Software, Inc.). $P \leq 0.05$ or $P \leq 0.001$ was considered to indicate a statistically significant difference.

Results

Production of an active recombinant hGC33-PE38 immunotoxin. The recombinant hGC33-PE38 immunotoxin generated in the present study displayed ~94% homogeneity and concentration of 9 mg/ml (Fig. 1).

An *in vitro* enzymatic activity of recombinant proteins was evaluated using a solid-phase assay against *S. cerevisiae* eEF2 as a substrate, as previously described (43). The calculated EC_{50} values for hGC33-PE38 and N-PE38 were nearly the same (Table I), suggesting that the enzymatic activity of the hGC33-PE38 was comparable to the wild type of the N-PE38 toxin.

The affinity of the hGC33-PE38 immunotoxin to GPC3 was determined by ELISA. The immunoreactivity of hGC33-PE38 was analysed for 1 $\mu\text{g/ml}$ of protein against GPC3 antigen

Table I. ADP-ribosylation activity of N-PE38 and hGC33-PE38.

Toxin	EC ₅₀ , pmol/ml	95% CI
N-PE38	15.4	13.9-17
hGC33-PE38	15.2	13.7-16.5

n=3. N, native; PE38, *Pseudomonas aeruginosa* exotoxin A 38; hGC33, anti-GPC3 antibody.

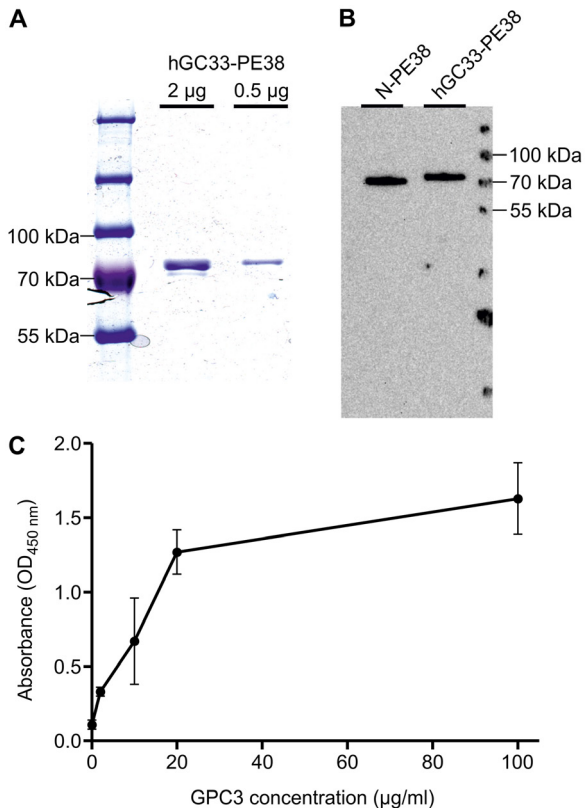


Figure 1. Molecular analysis of purified hGCPE38 and N-PE38. Proteins from pooled and concentrated size-exclusion chromatography fractions were loaded onto SDS-PAGE gels and analysed. (A) SDS-PAGE in reducing conditions: 2,000 or 500 ng of the hGCPE38 protein per lane. (B) Western blotting. The toxins were detected using anti-exotoxin A-specific primary antibodies; 50 ng of each protein per lane. (C) Enzyme-linked immunosorbent assay analysis of hGC33-PE38 binding affinity to GPC3 antigen. Absorbance values are given as the mean \pm SD from three independent replicates. BSA (0 μ g/ml of GPC3 antigen) was the negative control. PE38, *Pseudomonas aeruginosa* exotoxin A 38; hGC33, anti-GPC3 antibody; GPC3, glypican-3.

in five different concentrations (2-100 μ g/ml/well; Fig. 1). Observed absorbance values (OD_{450nm}) increased (0.22 \pm 0.03) even for the lowest concentration of GPC3 tested (2 μ g/ml) (Fig. 1), demonstrating that hGC33-PE38 can bind to GPC3 *in vitro*.

hGC33-PE38 internalisation. As a positive control for GPC3-directed immunotoxin uptake, HepG2 liver cancer cells were used. HepG2 is known to express GPC3 abundantly in the cell membrane and shows the ability to internalise anti-GPC3 immunotoxins at a high rate (39). For the protein-binding specificity evaluation, the A549 adenocarcinoma cell line

Table II. Cytotoxicity of hGC33-PE38 toward liver and lung cancer cell lines.

A, Liver cancer

Cell line	IC ₅₀ , mean \pm SD, ng/ml	P-value (vs. H446)
HepG2	330 \pm 15	P<0.0001
SNU-398	>1650	P<0.0001
SNU-449	No effect	P<0.0001

B, Lung cancer

Cell line	IC ₅₀ , mean \pm SD, ng/ml	P-value (vs. H446)
H446	70.6 \pm 4.6	-
H510A	No effect	P<0.0001
A549	No effect	P<0.0001
SK-MES1	No effect	P<0.0001

PE38, *Pseudomonas aeruginosa* exotoxin A 38; hGC33, anti-GPC3 antibody.

was also tested, chosen due to low/no GPC3 expression (30). As shown in Fig. 2, Alexa Fluor 488-labelled hGC33-PE38 is effectively internalised into HepG2 cells within 3 h. Fluorescence is clearly visible in the cytoplasm with especially high density of signal in globular clusters around the nuclei (Fig. 2). Untreated HepG2 control cells have not shown visible fluorescence in Alexa Fluor 488 specific channel (data not shown). No evident immunotoxin uptake was observed in the case of A549 cells. Control untreated A549 cells have also not shown visible fluorescence in Alexa Fluor 488 specific channel (data not shown). As these cells are generally capable of effectively internalising native exotoxin A and its variant in analogous experiments (43), these observations demonstrated that the internalisation of hGC33-PE38 was GPC3-dependent.

Additionally, the internalisation of ATTO 542-labelled hGC33-PE38 was tested on two SCLC lines, NCI-H510A and NCI-H446. The immunotoxin uptake was evident in the case of H446 cells (Fig. 3), resulting in strong, punctate/globular staining in the cytoplasm, while untreated NCI-H510A control cells have not shown visible fluorescence in ATTO 542 specific channel (data not shown). In contrast, ATTO 542-labelled hGC33-PE38 internalisation was not detected in NCI-H510A cells (Fig. 3) and ATTO-542-specific fluorescence was also not visible in untreated NCI-H510A control cells.

In vitro biological activity of hGC33-PE38. The biological activity of hGC33-PE38 was evaluated *in vitro* on cancer cell lines. Cytotoxicity was assessed after 48-h incubation with hGC33-PE38 in various concentrations by enumerating viable cells using a neutral red uptake assay (44). Preliminary analyses were performed on liver cancer cell lines as a model for anti-GPC3 immunotoxin potency validation. As a positive control, HepG2 cells, which express GPC3 at high levels, were tested. hGC33-PE38 was cytotoxic to HepG2 cells in a dose-dependent manner with an IC₅₀ of 330 \pm 15 ng/ml (Table II).

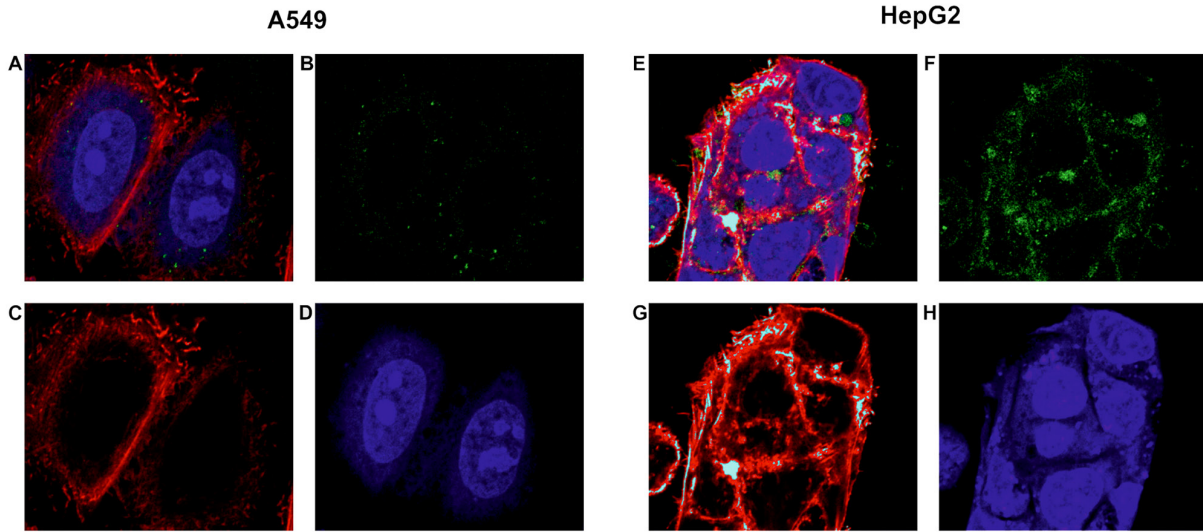


Figure 2. Internalisation of hGC33-PE38 immunotoxin in A549 and HepG2 cells visualised using confocal microscopy. Merged views are shown in parts A and E on both panels. Fluorescent signal corresponding to the hGC33-PE38 immunotoxin is marked as green (parts B and F). The cells were treated with fluorescently labelled hGC33-PE38 immunotoxin (Alexa Fluor 488), fixed and additionally labelled with Alexa Fluor 594 Phalloidin for actin visualisation (parts C and G), and with NucRed Live 647 Ready Probes Reagent (parts D and H) for nuclei visualisation. Magnification, x60. PE38, *Pseudomonas aeruginosa* exotoxin A 38; hGC33, anti-GPC3 antibody.

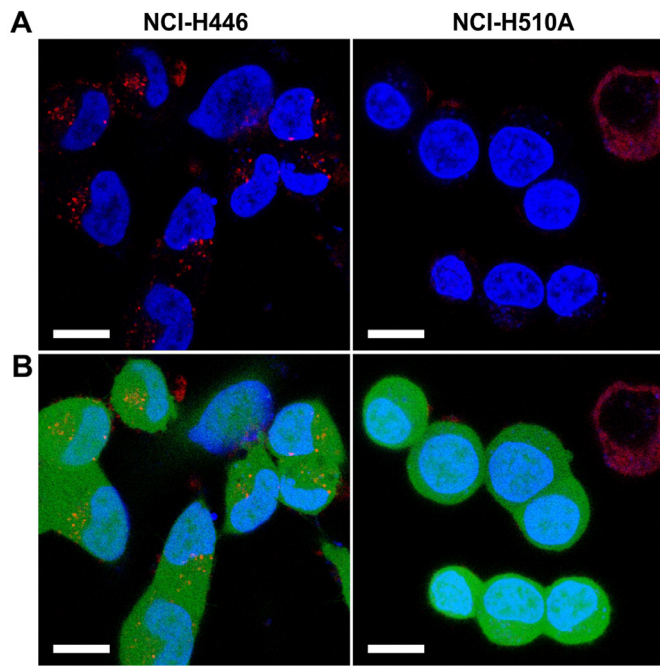


Figure 3. Internalisation of hGC33-PE38 immunotoxin in NCI-H446 and NCI-H510A cells visualised using confocal microscopy. Blue channel, nuclei (Hoechst 33342); green channel, live cells (calcein-AM); red channel, hGC33-PE38 (ATTO 542). (A) Intracellular localization of ATTO 542-stained hGC33-PE38 immunotoxin within NCI-H446 cells and no specific signal in NCI-H510A cells. (B) Calcein-AM staining indicates shape of the cells and tightness of cellular membrane. On the upper right corner of the right panels, non-specific binding within a dead cell is shown. Scale bar, 10 μ m. Magnification, x60. PE38, *Pseudomonas aeruginosa* exotoxin A 38; hGC33, anti-GPC3 antibody.

For specificity evaluation, the SNU-398 (low GPC3 expression) and SNU-449 (GPC3-null) lines were treated (47). As expected, no cytotoxicity in the SNU-449 cell line was observed, and only small yet detectable cytotoxicity (13% at the highest dose;

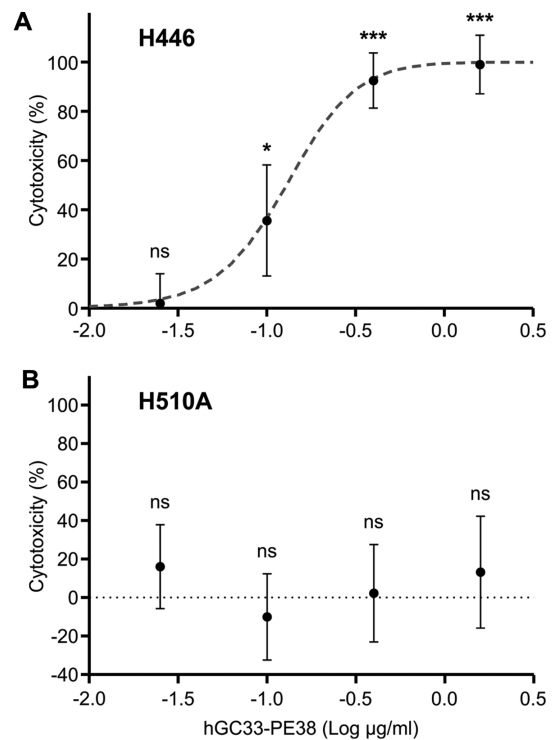


Figure 4. Treatment of H446 and H510A cells with increasing concentrations of the hGC33-PE38 immunotoxin. (A) Cytotoxicity curve for H446 cells. Dashed line represents the logarithmic dose-response logistic curve fitted to data. (B) No effect on H510A cells' survival. Dotted line represents the baseline of cytotoxicity. Cytotoxicity was calculated based on the analysis of neutral red uptake by viable cells. Mean \pm SD (n=3). Statistical significance of differences vs. control (fixed value, 0) was calculated with ANOVA and Dunnett's post hoc test; * $P \leq 0.05$, *** $P \leq 0.001$. PE38, *Pseudomonas aeruginosa* exotoxin A 38; hGC33, anti-GPC3 antibody.

data not shown) was seen in SNU-398 cells. These findings suggested that the cytotoxicity of hGC33-PE38 was specific and dependent on GPC3 expression levels on the target cells. The

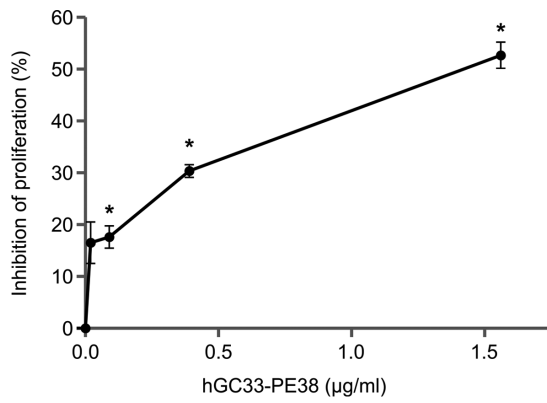


Figure 5. Inhibition of H446 cell proliferation treated for 48 h with increasing concentrations of the hGC33-PE38 immunotoxin. Proliferation inhibition was determined using the BrdU assay. Mean \pm SD (n=3). Statistical significance of differences vs. control (point 0.0) was calculated with ANOVA and Tukey's post hoc test; * $P \leq 0.05$. PE38, *Pseudomonas aeruginosa* exotoxin A 38; hGC33, anti-GPC3 antibody.

SCLC cell lines tested were chosen based on microarray results obtained previously by Klijn *et al* (41). Two SCLC lines with the highest levels of GPC3 expression were tested for immunotoxin cytotoxicity, NCI-H510A and NCI-H446. Despite expressing similar levels of GPC3 mRNA, the responses of these lines to hGC33-PE38 immunotoxin differed. The H446 line was sensitive to hGC33-PE38 in a dose-dependent manner, and the IC_{50} for the immunotoxin was 70.6 ± 4.6 ng/ml (Table II and Fig. 4). However, for H510A, no cytotoxicity was observed even at the highest tested concentration (1,562 ng/ml). Additionally, two lung cancer lines with previously reported low or undetectable GPC3 expression were analysed. The A549 LAD cells were insensitive to hGC33-PE38 even at a 1,600 ng/ml dose (the highest tested) (Table II). The second GPC3-negative cell line to be tested was the SK-MES-1 LSCC cell line (30). The SK-MES-1 cells were resistant to hGC33-PE38 and remained viable at the highest concentration of immunotoxin tested (1,650 ng/ml; Table II).

The anti-proliferative effect of hGC33-PE38 immunotoxin on NCI-H446 cells was evaluated using a BrdU assay. Cells were analysed 48 h after immunotoxin treatment. As shown in Fig. 5, hGC33-PE38 inhibits cell proliferation in dose-dependent manner. A 48-h incubation with 1.5 μ g/ml hGC33-PE38 resulted in inhibition of proliferation by ~50% in NCI-H446 cell culture.

Comparison of GPC3 and β -catenin expression in NCI-H446 and NCI-H510A cells. The SCLC cell lines in the present study were chosen based on microarray results obtained by Klijn *et al* (41). Analysis of the publicly available microarray results was performed for lung adenocarcinoma, lung adenocarcinoma, small cell lung carcinoma and squamous cell lung carcinoma lines. Of the 67 cell lines analysed, 20 SCLC lines and 9 LAD lines exhibited expression values above the cut-off (Fig. 6). Almost the same mRNA levels of GPC3 were reported for H446 and H510A lines (58 fragments per kilobase of exon model per million reads mapped for H510A and 59 for H446).

GPC3 mRNA levels were verified in both SCLC cell lines via RT-qPCR. The expression levels of GPC3 were comparable between NCI-H446 and NCI-H510A cells (Table III).

The transcript abundance of the β -catenin (CTNNB1 gene) was also measured in both SCLC lines. The expression of

Table III. Relative expression levels of the GPC3 and β -catenin genes in NCI-H446 and NCI-H510A cells.

Cell line	GPC3 expression mean \pm SD	β -catenin expression mean \pm SD
H446	919 \pm 470	50 \pm 44
H510A	955 \pm 180; P=0.886 (vs. H446)	26 \pm 9; P=0.629 (vs. H446)

GPC3, glypican-3.

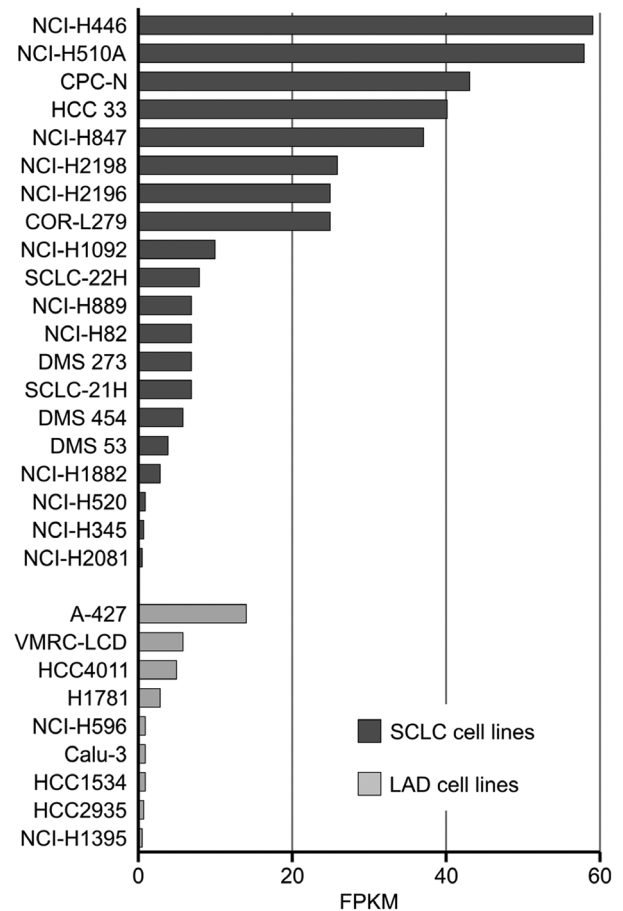


Figure 6. Graph showing a normalized estimation of the GPC3 gene expression across 67 lung cancer cell lines. Data obtained from the EMBL-EBI Expression Atlas tool. The x-axis presents expression values in FPKM. The accession number of primary dataset: E-MTAB-2706. LAD, lung adenocarcinoma; SCLC, small cell lung carcinoma; GPC3, glypican-3; FPKM, fragments per kilobase of exon model per million reads mapped.

β -catenin was detectable in both cell types. However, β -catenin levels were higher in NCI-H446, compared with NCI-H510A, although this trend was not statistically significant (Table III).

Treatment of NCI-H446 and NCI-H510A cells with hGC33-PE38 did not result in changes in expression of GPC3 and β -catenin (data not shown).

Surface-bound GPC3 detection. Due to the differences in hGC33-PE38 cytotoxicity on SCLC lines, despite their similar levels of GPC3 expression, the levels of cell surface-bound

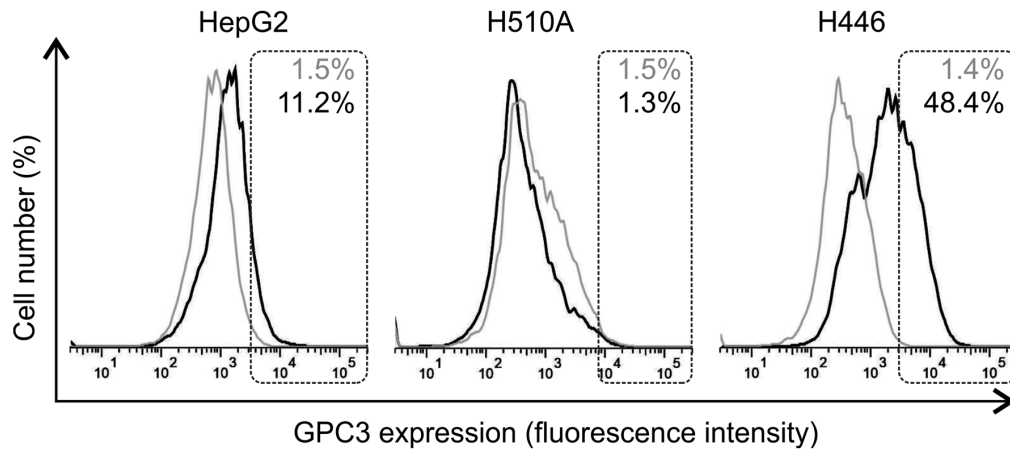


Figure 7. Cell surface expression of GPC3 in HepG2, H510A and H446 cell lines measured by flow cytometry. Grey curves/numbers on the histograms represent cell staining with isotype control; black curves/numbers represent cells stained by antibodies recognising GPC3. Boxes represent interval gates threshold based on respective isotype control. GPC3, glypican-3.

GPC3 were then examined in the H510A, H446 and HepG2 cell lines using flow cytometry. The results indicated varying levels of GPC3 surface expression in different tested cell lines. While H446 cells exhibited a strong positive staining with anti-GPC3 antibodies, H510A cells were GPC3-negative (Fig. 7). As previously reported by other authors, HepG2 cells showed GPC3-positive staining (Fig. 7). Interestingly, H446 cells exhibited a higher level of GPC3 specific immunoreactivity on their surface compared with HepG2 cells (Fig. 7).

Discussion

In the present study, a hGC33-PE38 immunotoxin targeting GPC3 was generated using the recombinant humanized monoclonal antibody hGC33. hGC33 has previously been demonstrated to inhibit HCC tumour growth via antibody-dependent cellular cytotoxicity (35,48,49). Cytotoxicity of the hGC33-PE38 was first evaluated against a panel of liver cancer cell lines employed as a model for GPC3-targeted cancer immunotherapy. The results confirmed the hypothesis that the hGC33-PE38 immunotoxin could kill GPC3-expressing cells (HepG2), but not cancer cells lacking surface expression of this antigen (SNU-449 line) and was only slightly cytotoxic to cells expressing GPC3 at low levels (SNU-398 line). The specificity of hGC33-PE38 was additionally confirmed by treating known GPC3-negative lung cancer cell lines. The hGC33 antibody could potentially serve as an alternative to HN3, developed by Feng *et al* (50), to create effective anti-GPC3 immunotoxins. Although not fully of human origin, hGC33 was well-tolerated in clinical trials (35,48,49). The antitumour potential of hGC33-PE38 should be further evaluated *in vivo*. However, the potential clinical use of hGC33-PE38 might be restricted due to the known immunogenicity of the PE38 molecule (51). Nonetheless, the present findings further support the potential use of GPC3 as a target in immunotherapy of SCLC.

The pathogenesis of SCLC is still unknown and the underlying molecular mechanism remains unclear (52). The potential role of the GPC3 protein in these processes might be of interest, due to its association with the Hh and Wnt/ β -catenin signalling pathways, which are considered as

contributing mechanisms in SCLC pathogenesis (45,53-56). Recently published data suggest the role of Wnt/ β -catenin pathway activation in chemotherapy resistance and SCLC relapse (56). Interestingly, Pan *et al* (45) demonstrated the inhibitory effect of XAV939 (a small-molecule inhibitor of the Wnt/ β -catenin signalling pathway) on the proliferation of NCI-H446 cells, suggesting inhibition of Wnt signalling as a potential therapeutic approach for advanced SCLC disease.

Previous studies on the pathogenesis of SCLC have described this disease as dynamic and involving diverse cellular and molecular processes (57-59). In the present study, two cancer lines were tested, NCI-H510A and NCI-H446. Both lines were isolated by Carney *et al* (60) in 1982 from male, adult patients, and both were derived from metastatic sites: H510A from adrenal metastasis and H446 from pleural effusion. On the basis of biochemical markers and morphological differences, the H510A cell line is a classic-SCLC line defined by upregulation of all four APUD (amine precursor uptake and decarboxylation) biomarkers (60,61). In contrast, H446 is a variant-SCLC line expressing only two biomarkers and presenting atypical morphology (60-63). Gazdor *et al* (62) suggested that the unique, variant phenotype of the H446 line manifests early in *in vitro* culture and reflects the morphology of the tumour of origin. Thus, it is not a result of changes occurring during culture. It is known that SCLC cells with variant morphologies have increased expression of the c-myc oncogene, shorter doubling time, decreased or absent expression of neuroendocrine cell features and can be resistant to conventional therapy (62-65). In the present study, the relatively high levels of GPC3 protein observed on the cell surface of the NCI-H446 line suggested that GPC3 could potentially act as an oncogene in these cells. The reason why GPC3 is almost undetectable on the surface of H510A cells despite the high expression observed at the mRNA level is unknown. The presence or absence of GPC3 on the surface of the H446 and H510A cells directly corresponded to their sensitivity to hGC33-PE38 immunotoxin. In the case of H446 cells, GPC3 acted as an antigen for the immunotoxin and enabled its internalisation, resulting in cytotoxicity. The observed cytotoxicity and anti-proliferative effects of the hGC33-PE38

immunotoxin on H446 cells were dose-dependent. To the best of our knowledge, this is the first demonstration of the use of GPC3 as a target for SCLC cell killing. Due to the known properties of GPC3, differences may be expected between H446 and H510A lines in signalling cascades that are important for SCLC initiation and progression. Importantly, the mRNA level of β -catenin was higher in H446 compared with H510A cells, although this trend was not statistically significant (Table III). Most probably, the H446 cell line represents the SCLC subtype with the active canonical Wnt/ β -catenin pathway enhanced by overexpressed, cell surface-bound GPC3. Recently, Wang *et al* (66) demonstrated that GPC3 promotes the progression of lung squamous cell carcinoma through upregulation of β -catenin expression. It is also known that in hepatocellular carcinoma, the GPI anchoring and the cell surface localization of GPC3 is needed for Wnt/ β -catenin signalling activation and cell proliferation (10,67).

It is thus conceivable that high surface expression of GPC3 in H446 cells can represent some important characteristics of late-stage SCLC, which is associated with high aggressiveness, and chemo- and/or radio-therapy resistance. This warrants further study of the potential oncogenic role of GPC3 in SCLC, particularly in the context of different stages of the disease.

In conclusion, the present study described the production and *in vitro* activity of hGC33-PE38, a PE38-based immunotoxin targeting the GPC3 antigen. Similar to anti-GPC3 immunotoxins described elsewhere, the hGC33-PE38 was effectively internalised and cytotoxic to HepG2 cells, and ineffective in the case of GPC3-negative cancer cells. A major focus of this study was the evaluation of hGC33-PE38 toxicity against cell lines representing cancer types that are not yet recognised as GPC3-associated. SCLC was considered as such, based on previous microarray results suggesting GPC3 gene upregulation. Two SCLC lines were chosen and treated with hGC33-PE38 in order to test GPC3-directed cytotoxicity. Despite similar GPC3 mRNA levels in both cell lines, only the H446 cell line was sensitive to hGC33-PE38, whereas H510A was resistant. This result was consistent with the difference in the amount of cell surface-bound GPC3 detected by flow cytometry. Since these cell lines were SCLC variants, the GPC3-associated phenotype reported here could reflect some important differences in the molecular pathways involved in diverse manifestations of the disease. Thus, cell surface-bound GPC3 might be considered as a potential target for SCLC therapy involving immunotoxins, other immunoconjugates or T cells. This hypothesis is consistent with recently reported activation of the Wnt/ β -catenin pathway in the advanced, chemo-resistant form of SCLC, and in line with ideas to treat advanced SCLC through inhibition of Wnt signalling. These observations also suggest a need for further studies of GPC3 cell-membrane abundance in different stages of SCLC.

Acknowledgements

The authors would like to thank Mrs. Isabelle Garcin and Professor Oliver Nüsse (University Paris-Sud, Orsay, France) for helping with confocal microscope imaging, and Professor Terri G. Kinzy (Robert Wood Johnson Medical School, Piscataway, NJ, USA) for providing the TKY675 mutant yeast strain for eEF2 production.

Funding

This study was supported by The Polish National Centre for Research and Development (grant no. pbs1/a9/16/2012).

Availability of data and materials

The datasets used and/or analyzed during the present study are available from the corresponding author on reasonable request.

Authors' contributions

AWD, MB, MG, JG, MiR, MaR and ER conducted the research, prepared and visualized the data, and performed statistical and computational analyses. ER formulated the research goals. AWD, JD, KG, LR provided substantial contributions to the design of the study. JD, KG and LR provided supervision and leadership for their research teams. ER and AWD prepared the original draft of manuscript. The manuscript review, corrections and editing were performed by ER, JD, AWD, KG, MG, MaR and LR. All authors read and approved the final version of manuscript.

Ethics approval and consent to participate

Not applicable.

Patient consent for publication

Not applicable.

Competing interests

The authors declare that they have no competing interests.

References

1. Haruyama Y and Kataoka H: Glypican-3 is a prognostic factor and an immunotherapeutic target in hepatocellular carcinoma. *World J Gastroenterol* 22: 275-283, 2016.
2. Fransson LA: Glypicans. *Int J Biochem Cell Biol* 35: 125-129, 2003.
3. Filmus J, Shi W, Wong ZM and Wong MJ: Identification of a new membrane-bound heparan sulphate proteoglycan. *Biochem J* 311: 561-565, 1995.
4. De Cat B, Muyldermans SY, Coomans C, Degeest G, Vanderschueren B, Creemers J, Biemar F, Peers B and David G: Processing by proprotein convertases is required for glypican-3 modulation of cell survival, Wnt signaling, and gastrulation movements. *J Cell Biol* 163: 625-635, 2003.
5. Iglesias BV, Centeno G, Pascuccelli H, Ward F, Peters MG, Filmus J, Puricelli L and de Kier Joffé EB: Expression pattern of glypican-3 (GPC3) during human embryonic and fetal development. *Histol Histopathol* 23: 1333-1340, 2008.
6. Hsu HC, Cheng W and Lai PL: Cloning and expression of a developmentally regulated transcript MXR7 in hepatocellular carcinoma: Biological significance and temporospatial distribution. *Cancer Res* 57: 5179-5184, 1997.
7. Ho M and Kim H: Glypican-3: A new target for cancer immunotherapy. *Eur J Cancer* 47: 333-338, 2011.
8. Li J, Gao JZ, Du JL and Wei LX: Prognostic and clinicopathological significance of glypican-3 overexpression in hepatocellular carcinoma: A meta-analysis. *World J Gastroenterol* 20: 6336-6344, 2014.
9. Liu JW, Zuo XL and Wang S: Diagnosis accuracy of serum Glypican-3 level in patients with hepatocellular carcinoma and liver cirrhosis: A meta-analysis. *Eur Rev Med Pharmacol Sci* 19: 3655-3673, 2015.

10. Capurro MI, Xiang YY, Lobe C and Filmus J: Glypican-3 promotes the growth of hepatocellular carcinoma by stimulating canonical Wnt signaling. *Cancer Res* 65: 6245-6254, 2005.
11. Kolluri A and Ho M: The role of glypican-3 in regulating Wnt, Yap, and Hedgehog in liver cancer. *Front Oncol* 9: 708, 2019.
12. Filmus J and Capurro M: The role of glypican-3 in the regulation of body size and cancer. *Cell Cycle* 7: 2787-2790, 2008.
13. Saikali Z and Sinnett D: Expression of glypican 3 (GPC3) in embryonal tumors. *Int J Cancer* 89: 418-422, 2000.
14. Ota S, Hishinuma M, Yamauchi N, Goto A, Morikawa T, Fujimura T, Kitamura T, Kodama T, Aburatani H and Fukayama M: Oncofetal protein glypican-3 in testicular germ-cell tumor. *Virchows Arch* 449: 308-314, 2006.
15. Yamanaka K, Ito Y, Okuyama N, Noda K, Matsumoto H, Yoshida H, Miyauchi A, Capurro M, Filmus J and Miyoshi E: Immunohistochemical study of glypican 3 in thyroid cancer. *Oncology* 73: 389-394, 2007.
16. Baumhoer D, Tornillo L, Stadlmann S, Roncalli M, Diamantis EK and Terracciano LM: Glypican 3 expression in human nonneoplastic, preneoplastic, and neoplastic tissues: A tissue microarray analysis of 4,387 tissue samples. *Am J Clin Pathol* 129: 899-906, 2008.
17. Zynger DL, Everton MJ, Dimov ND, Chou PM and Yang XJ: Expression of glypican 3 in ovarian and extragonadal germ cell tumors. *Am J Clin Pathol* 130: 224-230, 2008.
18. Cao D, Li J, Guo CC, Allan RW and Humphrey PA: SALL4 is a novel diagnostic marker for testicular germ cell tumors. *Am J Surg Pathol* 33: 1065-1077, 2009.
19. Wang F, Liu A, Peng Y, Rakheja D, Wei L, Xue D, Allan RW, Molberg KH, Li J and Cao D: Diagnostic utility of SALL4 in extragonadal yolk sac tumors: An immunohistochemical study of 59 cases with comparison to placental-like alkaline phosphatase, alpha-fetoprotein, and glypican-3. *Am J Surg Pathol* 33: 1529-1539, 2009.
20. Ikeda H, Sato Y, Yoneda N, Harada K, Sasaki M, Kitamura S, Sudo Y, Ooi A and Nakanuma Y: α -Fetoprotein-producing gastric carcinoma and combined hepatocellular and cholangiocarcinoma show similar morphology but different histogenesis with respect to SALL4 expression. *Hum Pathol* 43: 1955-1963, 2012.
21. Aydin O, Yildiz L, Baris S, Dundar C and Karagoz F: Expression of Glypican 3 in low and high grade urothelial carcinomas. *Diagn Pathol* 10: 34, 2015.
22. Nguyen T, Phillips D, Jain D, Torbenonson M, Wu TT, Yeh MM and Kakar S: Comparison of 5 immunohistochemical markers of hepatocellular differentiation for the diagnosis of hepatocellular carcinoma. *Arch Pathol Lab Med* 139: 1028-1034, 2015.
23. Foda AA, Mohammad MA, Abdel-Aziz A and El-Hawary AK: Relation of glypican-3 and E-cadherin expressions to clinicopathological features and prognosis of mucinous and non-mucinous colorectal adenocarcinoma. *Tumour Biol* 36: 4671-4679, 2015.
24. Yu X, Li Y, Chen SW, Shi Y and Xu F: Differential expression of glypican-3 (GPC3) in lung squamous cell carcinoma and lung adenocarcinoma and its clinical significance. *Genet Mol Res* 14: 10185-10192, 2015.
25. Ortiz MV, Roberts SS, Glade Bender J, Shukla N and Wexler LH: Immunotherapeutic targeting of GPC3 in pediatric solid embryonal tumors. *Front Oncol* 9: 108, 2019.
26. Murthy SS, Shen T, De Rienzo A, Lee WC, Ferriola PC, Jhanwar SC, Mossman BT, Filmus J and Testa JR: Expression of GPC3, an X-linked recessive overgrowth gene, is silenced in malignant mesothelioma. *Oncogene* 19: 410-416, 2000.
27. Xiang YY, Ladeda V and Filmus J: Glypican-3 expression is silenced in human breast cancer. *Oncogene* 20: 7408-7412, 2001.
28. Peters MG, Farías E, Colombo L, Filmus J, Puricelli L and Bal de Kier Joffé E: Inhibition of invasion and metastasis by glypican-3 in a syngeneic breast cancer model. *Breast Cancer Res Treat* 80: 221-232, 2003.
29. Valsechi MC, Oliveira AB, Conceição AL, Stuuqui B, Candido NM, Provazzi PJ, de Araújo LF, Silva WA Jr, Calmon MF and Rahal P: GPC3 reduces cell proliferation in renal carcinoma cell lines. *BMC Cancer* 14: 631, 2014.
30. Kim H, Xu GL, Borczuk AC, Busch S, Filmus J, Capurro M, Brody JS, Lange J, D'Armiento JM, Rothman PB, *et al*: The heparan sulfate proteoglycan GPC3 is a potential lung tumor suppressor. *Am J Respir Cell Mol Biol* 29: 694-701, 2003.
31. Aviel-Ronen S, Lau SK, Pintilie M, Lau D, Liu N, Tsao MS and Jothy S: Glypican-3 is overexpressed in lung squamous cell carcinoma, but not in adenocarcinoma. *Mod Pathol* 21: 817-825, 2008.
32. Lin Q, Xiong LW, Pan XF, Gen JF, Bao GL, Sha HF, Feng JX, Ji CY and Chen M: Expression of GPC3 protein and its significance in lung squamous cell carcinoma. *Med Oncol* 29: 663-669, 2012.
33. Li K, Pan X, Bi Y, Xu W, Chen C, Gao H, Shi B, Jiang H, Yang S, Jiang L, *et al*: Adoptive immunotherapy using T lymphocytes redirected to glypican-3 for the treatment of lung squamous cell carcinoma. *Oncotarget* 7: 2496-2507, 2016.
34. Jiang Z, Jiang X, Chen S, Lai Y, Wei X, Li B, Lin S, Wang S, Wu Q, Liang Q, *et al*: Anti-GPC3-CAR T Cells Suppress the Growth of Tumor Cells in Patient-Derived Xenografts of Hepatocellular Carcinoma. *Front Immunol* 7: 690, 2017.
35. Nakano K, Ishiguro T, Konishi H, Tanaka M, Sugimoto M, Sugo I, Igawa T, Tsunoda H, Kinoshita Y, Habu K, *et al*: Generation of a humanized anti-glypican 3 antibody by CDR grafting and stability optimization. *Anticancer Drugs* 21: 907-916, 2010.
36. Brinkmann U: Recombinant immunotoxins: Protein engineering for cancer therapy. *Mol Med Today* 2: 439-446, 1996.
37. Pastan I, Hassan R, Fitzgerald DJ and Kreitman RJ: Immunotoxin therapy of cancer. *Nat Rev Cancer* 6: 559-565, 2006.
38. Shapira A and Benhar I: Toxin-based therapeutic approaches. *Toxins (Basel)* 2: 2519-2583, 2010.
39. Gao W, Tang Z, Zhang YF, Feng M, Qian M, Dimitrov DS and Ho M: Immunotoxin targeting glypican-3 regresses liver cancer via dual inhibition of Wnt signalling and protein synthesis. *Nat Commun* 6: 6536, 2015.
40. Wang C, Gao W, Feng M, Pastan I and Ho M: Construction of an immunotoxin, HN3-mPE24, targeting glypican-3 for liver cancer therapy. *Oncotarget* 8: 32450-32460, 2017.
41. Klijn C, Durinck S, Stawiski EW, Haverty PM, Jiang Z, Liu H, Degenhardt J, Mayba O, Gnad F, Liu J, *et al*: A comprehensive transcriptional portrait of human cancer cell lines. *Nat Biotechnol* 33: 306-312, 2015.
42. Weldon JE and Pastan I: A guide to taming a toxin--recombinant immunotoxins constructed from Pseudomonas exotoxin A for the treatment of cancer. *FEBS J* 278: 4683-4700, 2011.
43. Borowiec M, Gorzkiewicz M, Grzesik J, Walczak-Drzewiecka A, Salkowska A, Rodakowska E, Steczkiewicz K, Rychlewski L, Dastyk J and Ginalski K: Towards Engineering Novel PE-Based Immunotoxins by Targeting Them to the Nucleus. *Toxins (Basel)* 8: 321, 2016.
44. Repetto G, del Peso A and Zurita JL: Neutral red uptake assay for the estimation of cell viability/cytotoxicity. *Nat Protoc* 3: 1125-1131, 2008.
45. Pan F, Shen F, Yang L, Zhang L, Guo W and Tian J: Inhibitory effects of XAV939 on the proliferation of small-cell lung cancer H446 cells and Wnt/ β -catenin signaling pathway *in vitro*. *Oncol Lett* 16: 1953-1958, 2018.
46. Vandesompele J, De Preter K, Pattyn F, Poppe B, Van Roy N, De Paepe A and Speleman F: Accurate normalization of real-time quantitative RT-PCR data by geometric averaging of multiple internal control genes. *Genome Biol* 3: research0034.1, 2002.
47. Sun Ck, Chua Ms, Wei W and So S: Glypican-3-Mediates Autophagy and Promotes Self-Renewal and Tumor Initiation of Hepatocellular Carcinoma Cells. *Biol J Stem Cell Res Ther* 4: 9, 2014.
48. Ishiguro T, Sugimoto M, Kinoshita Y, Miyazaki Y, Nakano K, Tsunoda H, Sugo I, Ohizumi I, Aburatani H, Hamakubo T, *et al*: Anti-glypican 3 antibody as a potential antitumor agent for human liver cancer. *Cancer Res* 68: 9832-9838, 2008.
49. Yen CJ, Daniele B, Kudo M, Merle P, Park JW, Ross P, Péron JO, Ebert O, Chan S, Poon RT, *et al*: Randomized phase II trial of intravenous RO5137382/GC33 at 1600 mg every other week and placebo in previously treated patients with unresectable advanced hepatocellular carcinoma. *J Clin Oncol* 32 (Suppl 5): 4102a, 2014.
50. Feng M, Gao W, Wang R, Chen W, Man YG, Figg WD, Wang XW, Dimitrov DS and Ho M: Therapeutically targeting glypican-3 via a conformation-specific single-domain antibody in hepatocellular carcinoma. *Proc Natl Acad Sci USA* 110: E1083-E1091, 2013.
51. FitzGerald DJ, Wayne AS, Kreitman RJ and Pastan I: Treatment of hematologic malignancies with immunotoxins and antibody-drug conjugates. *Cancer Res* 71: 6300-6309, 2011.
52. Schulze AB, Evers G, Kerkhoff A, Mohr M, Schliemann C, Berdel WE and Schmidt LH: Future Options of Molecular-Targeted Therapy in Small Cell Lung Cancer. *Cancers (Basel)* 11: 690, 2019.

53. Watkins DN, Berman DM, Burkholder SG, Wang B, Beachy PA and Baylin SB: Hedgehog signalling within airway epithelial progenitors and in small-cell lung cancer. *Nature* 422: 313-317, 2003.
54. Park KS, Martelotto LG, Peifer M, Sos ml, Karnezis AN, Mahjoub MR, Bernard K, Conklin JF, Szczepny A, Yuan J, *et al*: A crucial requirement for Hedgehog signaling in small cell lung cancer. *Nat Med* 17: 1504-1508, 2011.
55. Szczepny A, Rogers S, Jayasekara WSN, Park K, McCloy RA, Cochrane CR, Ganju V, Cooper WA, Sage J, Peacock CD, *et al*: The role of canonical and non-canonical Hedgehog signaling in tumor progression in a mouse model of small cell lung cancer. *Oncogene* 36: 5544-5550, 2017.
56. Wagner AH, Devarakonda S, Skidmore ZL, Krysiak K, Ramu A, Trani L, Kunisaki J, Masood A, Waqar SN, Spies NC, *et al*: Recurrent WNT pathway alterations are frequent in relapsed small cell lung cancer. *Nat Commun* 9: 3787, 2018.
57. Borromeo MD, Savage TK, Kollipara RK, He M, Augustyn A, Osborne JK, Girard L, Minna JD, Gazdar AF, Cobb MH, *et al*: ASCL1 and NEUROD1 Reveal Heterogeneity in Pulmonary Neuroendocrine Tumors and Regulate Distinct Genetic Programs. *Cell Rep* 16: 1259-1272, 2016.
58. Poirier JT, Gardner EE, Connis N, Moreira AL, de Stanchina E, Hann CL and Rudin CM: DNA methylation in small cell lung cancer defines distinct disease subtypes and correlates with high expression of EZH2. *Oncogene* 34: 5869-5878, 2015.
59. Esteller L, Hernández S, Lopez-Rios F and Remon J: Could WNT inhibitors really knock on the treatment door of small cell lung cancer? *J Thorac Dis* 11 (Suppl 3): S381-S384, 2019.
60. Carney DN, Gazdar AF, Bepler G, Guccion JG, Marangos PJ, Moody TW, Zweig MH and Minna JD: Establishment and identification of small cell lung cancer cell lines having classic and variant features. *Cancer Res* 45: 2913-2923, 1985.
61. Carney DN, Gazdar AF, Nau M and Minna JD: Biological heterogeneity of small cell lung cancer. *Semin Oncol* 12: 289-303, 1985.
62. Gazdar AF, Carney DN, Nau MM and Minna JD: Characterization of variant subclasses of cell lines derived from small cell lung cancer having distinctive biochemical, morphological, and growth properties. *Cancer Res* 45: 2924-2930, 1985.
63. Zhang Z, Zhou Y, Qian H, Shao G, Lu X, Chen Q, Sun X, Chen D, Yin R, Zhu H, *et al*: Stemness and inducing differentiation of small cell lung cancer NCI-H446 cells. *Cell Death Dis* 4: e633, 2013.
64. Zhang W, Girard L, Zhang YA, Haruki T, Papari-Zareei M, Stastny V, Ghayee HK, Pacak K, Oliver TG, Minna JD, *et al*: Small cell lung cancer tumors and preclinical models display heterogeneity of neuroendocrine phenotypes. *Transl Lung Cancer Res* 7: 32-49, 2018.
65. Carney DN, Mitchell JB and Kinsella TJ: In vitro radiation and chemotherapy sensitivity of established cell lines of human small cell lung cancer and its large cell morphological variants. *Cancer Res* 43: 2806-2811, 1983.
66. Wang D, Gao Y, Zhang Y, Wang L and Chen G: Glypican-3 promotes cell proliferation and tumorigenesis through up-regulation of β -catenin expression in lung squamous cell carcinoma. *Biosci Rep* 39: BSR20181147, 2019.
67. Gao W and Ho M: The role of glypican-3 in regulating Wnt in hepatocellular carcinomas. *Cancer Rep* 1: 14-19, 2011.



This work is licensed under a Creative Commons Attribution-NonCommercial-NoDerivatives 4.0 International (CC BY-NC-ND 4.0) License.